

1 Article

# 2 Monitoring the wear trend in wind turbines by tracking the 3 Fourier vibration spectrum and base density support vector 4 machine

5 Claudiu Bisu <sup>1</sup>, Adrian Olaru <sup>1\*</sup>, Serban Olaru <sup>2</sup>, Adrian Alexei <sup>2</sup>, Niculae Mihai <sup>3</sup>, Haleema Ushaq <sup>1</sup>

6 <sup>1</sup> National University of Science and Technology POLITEHNICA Bucharest; claudiu.bisu@upb.ro;

7 <sup>1</sup> National University of Science and Technology POLITEHNICA Bucharest; aolaru\_51@ymail.com;

8 <sup>1</sup> National University of Science and Technology POLITEHNICA Bucharest; haleemaushaq71@gmail.com;

9 <sup>2</sup> Military Equipment and Technology Research Agency; serban1978@yahoo.com, alexei\_adrian@hotmail.com;

10 <sup>3</sup> Concordia Technical University, Montreal, Canada; mniculae@yahoo.com;

11 \* Correspondence: aolaru\_51@ymail.com; Tel.: +40723852628;


12  
13 **Abstract:** To make wind power more competitive, it is necessary to reduce turbine downtime and  
14 reduce costs associated with wind turbine Operation and Maintenance (O&M). Incorporating  
15 machine learning in developing condition-based predictive maintenance methodologies for wind  
16 turbines can enhance their efficiency and reliability. This paper presents a monitoring method that  
17 utilizes Base Density for the Support Vector Machine (BDSVM) and the evolutionary Fourier  
18 spectra of vibrations. This method allows smart monitoring of the function evolution of the  
19 turbine. A complex optimal function (FO) for 5-degree order has been developed that will be the  
20 boundary function of the BDSVM to timely determined from the Fourier spectrum by the  
21 magnitude- frequency, and place of the failure occurring in wind turbine drive. Trend of the  
22 failure was constructed with the maximal values of the frequency optimal functions for each of  
23 cases the upwind and downwind part of the gear box.

24 **Keywords:** wind turbine; monitoring; wear trend; Fourier vibration spectrum; support vector  
25 machine; base density of the collected data; machine learning.  
26

## 27 1. Introduction

### 28 1.1. The future of wind turbines and the novelty of the paper

29 Wind energy has seen remarkable growth over the past decade and continues to be  
30 on an upward trend in the power generation industry. In the current context of the  
31 reduction and even abandonment of conventional energy sources, wind energy becomes  
a basic source, along with nuclear and hydro. In these conditions, the reliability and  
stability of the operation are necessary to maintain the production capacity for the  
longest possible periods and with the best possible predictability [1]. With the rapid  
development of the wind turbine technology and according with a higher demand of  
renewable energy the number of wind turbine (WT) units had a major increase, but  
under these conditions the failure rate also increased [2]. Power transmission is  
influenced by all components in the kinematic chain, rotor, gearbox, and generator.  
After an experience of over 20 years, both in operation and research, it can be concluded  
that the component with the highest level of vulnerability is the gearbox, with a very  
high failure and downtime [1-3]. To make wind power more competitive, it is necessary  
to reduce turbine downtime and increase reliability. Condition monitoring can help  
reduce the chances of catastrophic failures, enabling cost-effective operation and

<b>Citation:</b> To be added by editorial staff during production.	32
Academic Editor: Firstname Lastname	33
Received: date	34
Revised: date	35
Accepted: date	36
Published: date	37
	38
<b>Copyright:</b> © 2023 by the authors. Submitted for possible open access publication under the terms and conditions of the Creative Commons Attribution (CC BY) license ( <a href="https://creativecommons.org/licenses/by/4.0/">https://creativecommons.org/licenses/by/4.0/</a> ).	39 40 41 42 43

44 maintenance practices. Compared to other applications, the representatives of the wind  
45 industry recognized quite late, the benefits and importance of monitoring the operating  
46 status through the use of artificial intelligence (AI) and vibration analysis [4]. Substantial  
47 research has been conducted to establish algorithms based on a large volume of data  
48 that train on specific moments of failure, through machine learning to obtain specific  
49 failure models [4-5].

50 This paper presents a method that leverages Fourier spectrum analysis and  
51 machine learning-based data extraction techniques for predicting wear in wind turbine  
52 operation. The novelty of the applied method lies in its utilization of unlabeled and  
53 uncategorized data to infer meaningful results for the predictive maintenance of wind  
54 turbines. In this study functions representing the vibration trends of turbines across  
55 certain speed parameters, power levels, and wind flow conditions have been  
56 constructed. Furthermore, a density-based data filtering technique drawn from a  
57 machine learning-based method; Based Density Support Vector Machines (BDSVM) has  
58 been employed at the data acquisition stages of the experiments.

59 The research was carried out over a period of about two months. The Fourier  
60 spectrum was analyzed at different points in time while maintaining regulated and  
61 controlled parameters. With the help of at least 5 points from the Fourier spectrum, the  
62 objective functions were defined. The evolution over time of these Fourier spectra's  
63 maximum points (amplitude-frequency) offers an effective approach to ensure  
64 predictive maintenance. The established objective functions can be utilized to determine  
65 the wear evolution in both the low-frequency and high-frequency areas of a wind  
66 turbine. As a result of the experiments the envelope of normal operation and the  
67 envelope of maximum limit of operation are obtained for the gearbox, which is the most  
68 vulnerable part of the wind turbine. The envelope of a maximum limit of operation  
69 refers to wind turbine operation until the appearance of a defect. These experiments  
70 define the frequency-amplitude limits, which allow predictive maintenance of turbine  
71 components by setting the intervention thresholds without the need for extensive data  
72 collection.

73 The organization of the paper is as follows. Section 1 includes the details of the  
74 current scenario of predictive maintenance of wind turbines and the state-of-the-art  
75 methods used for the condition monitoring of wind turbines. The research methods and  
76 experiments conducted in this study are discussed in Section 2. The results of the  
77 experiments and their interpretations are presented in Section 3 and the conclusion and  
78 future work is briefed in Section 4.

### 79 80 *1.2. Overview of wind turbine condition monitoring and its need*

81 Wind energy has seen remarkable growth over the past decade and continues to be on  
82 an upward trend in the power generation industry [3]. In the current context of the  
83 reduction and even abandonment of conventional energy sources, wind energy emerges  
84 as a primary source, along with nuclear energy and hydropower [5]. In these conditions,  
85 the reliability and stability of the wind turbine operations are crucial to maintaining the  
86 production capacity for prolonged periods and with optimal predictability [1].

87 The monitoring of wind turbine (WT) condition is defined as a complex process of  
88 monitoring the parameters of the state of the machine so that a significant change is  
89 detected, which indicates a possible developing fault [6]. This can potentially help in  
90 different stage of wear: early detection of incipient failures, thus reducing the chances of  
91 catastrophic failures, accurately assessing the proper functioning of the components and  
92 reducing maintenance costs, the analysis of the fundamental causes of the occurrence of  
93 defects and can ensure the optimal determination of the input parameters for an  
94 improved operation of the turbine, the establishment of the control strategy as well as  
95 the optimal design of the components [7-10]. In a broad sense, the CMS of a wind

turbine can target almost all of its major subsystems, including blades, nacelle, power transmission, tower, and foundation [9]. This paper presents a method that focuses on the monitoring of wind turbine, and can be applied to the different components of the wind turbine: rotor shaft with main bearings, gearbox, and generator. From a CMS perspective, the three major monitored transmission components are the rotor shaft, the gearbox, and the generator. Of these three components the gearbox causes the longest downtime [11-13]. For this reason, the gearbox was chosen as the main subsystem targeted in this study. In detail, this paper will cover the typical practices, challenges, and future research opportunities related to CM wind turbine drivetrains [14].

To understand the dynamic behaviour of a WT and especially of a planetary gearbox, a number of techniques have been used in research and in industrial field: vibration analysis, oil condition analysis, thermography, acoustic measurement, acoustic, boroscopic inspection, electrical parameters effects, self-diagnostic of sensors, etc [15]. In order to ensure optimal conditions for predictive maintenance, a combination of different techniques is needed. Even if the vibration technique has a dominant proportion, it is supported in the decision by the other specific technologies.

However, vibration analysis on component fault diagnosis in wind turbines is a hard challenge due to the complex mechanical conditions of the power transmission kinematic chain, the variable operating conditions with transient phenomena, and the speed differences between the different elements of the gearbox [15-17]. The use of vibration transducers, respectively piezoelectric accelerometers, is the most used method, with different sensitivities depending on the speed and with rigid fixation on the structure of the components [7-9]. The repartition of the sensors in the monitoring process of the wind turbine from the actual stage of the research is shown in Figure 1 and Table 1.

In this paper, the focus is on the monitoring of wind turbine drivetrains. The drive trains consist of the main bearing, main shaft, gearbox, brake, generator shaft, and generator. From a CM perspective, the three major monitored transmission components are the main bearing, the gearbox, and the generator. Of these three components [6] the gearbox causes the longest downtime. Other research has also shown that the gearbox is the most expensive subsystem to maintain during the 20-year operating life of a turbine [1-7]. For this reason, the gearbox was chosen as the main subsystem targeted in this study.

### 1.3. State of the Art in Turbine Wear Monitoring and Trend Analysis

Current research has led to the identification of the following monitoring techniques and directions, which can be applied to wind turbines [14-15]: Vibration analysis; Oil condition analysis; Thermography of important elements in the turbine structure (gearbox); Analysis of the physical condition of the materials; Measurement of elastic yielding and deformation of various components; Acoustic measurements in various sensitive areas of the turbine; Measurement of various electrical effects; Process parameter measurement; Visual inspection; Performance monitoring by comparing output sizes for the same input data; Use of self-diagnostic sensors (figure 1).

a) *Vibration analysis*- Vibration analysis is the most well-known technology for monitoring the working conditions, especially for rotating equipment [15]. The type of sensors used depends: on the frequency range used for monitoring, position of transducers on the transmission chain for the low-frequency range, velocity sensor in the 5- 1000 Hz frequency domain, accelerometers for the high-frequency range; acoustic sensor for gearbox monitoring or blades.

b) *Oil analysis* - Oil analysis is another evaluation criterion, which, coupled with vibration analysis, contributes to decision-making in predictive maintenance. Oil

146 analysis is mostly done offline, by sampling but also ensuring the quality of the oil,  
147 contamination with dirt from the parts in contact, moisture, degradation of additives  
148 and maintaining the oil filter. However, to protect oil quality, the application of online  
149 sensors is used more and more often, especially for particle counter. In addition,  
150 protecting the condition of the oil filter is currently mainly applied to both hydraulic oil  
151 and lubricating oil. In case of excessive pollution of the filter, or change in the  
152 characteristics of the oil, this leads to excessive wear [15].

153 c) *Thermography*- Thermography is often applied for monitoring and fault identification  
154 of electrical and electronic components [15]. Hot spots due to component degeneration  
155 or poor contacts can be identified in a simple and fast way by using cameras and  
156 diagnostic software. Mainly they are used in generator and power converter monitoring  
157 but also for the thermal gear contact.

158 d) *Inspection of components condition*- This type of monitoring mainly focuses on detecting  
159 and tracking the evolution of wear, using boroscope device. The methods are normally  
160 offline and are a very important decision criterion for stopping, limiting or planning the  
161 repair [15-16].

162 e) *Deformation measurement*- Deformation measurement using manometers is a common  
163 technique but not often applied in a case of wind turbine monitoring. Strain gauges are  
164 not robust in the long term [15-17]. For wind turbines, deformation measurement can be  
165 very useful for life prediction and stress level protection, especially for blades [18] and  
166 also for the main shaft.

167 f) *Acoustic monitoring* - Acoustic monitoring is related to vibration monitoring using the  
168 noise measurement. Acoustic monitoring technology can be used for blades condition  
169 monitoring using acoustic microphone or for bearings and gearboxes monitoring using  
170 acoustic emission sensor fixed directly to the housing [15].

171 g) *Electrical effects* – Electrical parameters monitoring of generator represent a mandatory  
172 condition in based condition maintenance (CBM). The analysis of electrical parameters,  
173 such as: electrical current, voltage, insulation, power, etc., they allow both the evaluation  
174 of the quality of the generated power and the analysis of the potential faults [17].

175 h) *Process parameters*- Control systems monitoring (CMS) are becoming more  
176 sophisticated and their diagnostic capabilities are improving. However, protection is  
177 mostly based on level detection or signal comparison, which directly leads to an alarm  
178 when the signals exceed predefined threshold values. The integration of machine learning  
179 is still at the beginning, but in the future, solutions using AI will be sought for the large-  
180 scale development [15].

181 i) *Performance monitoring*- Wind turbine performance is often gauged through the  
182 relationship between power, wind speed, rotor speed, and blade angle, and in case of  
183 large deviations, an alarm or even stopping is generated [15]. Detection of margins are  
184 large to prevent false alarms [19]. Similar to process parameter estimation, more  
185 sophisticated methods like performance evolution monitoring are still not a common  
186 practice.

187 Thus, to obtain reliable predictive maintenance results, a combination of different  
188 techniques is needed. While vibration analysis may hold a predominant role, it is  
189 complemented by other specific technologies to perform decision-making accurately  
190 (figure 1).  
191

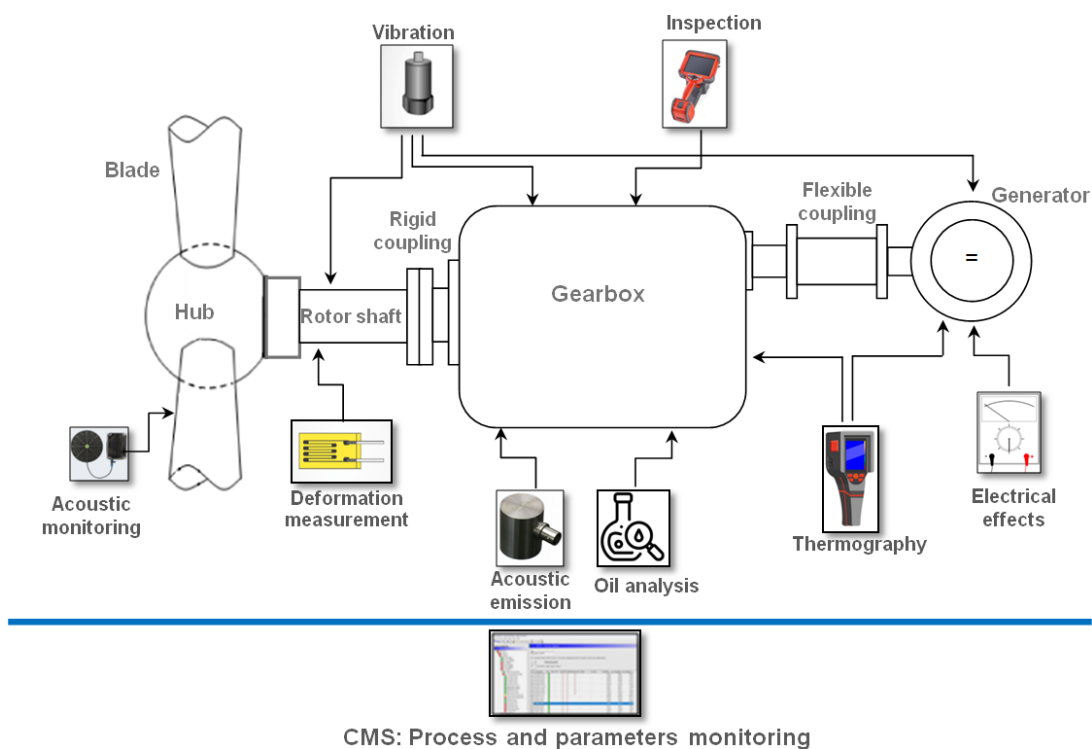


Figure 1. The position of the sensors for the monitoring process.

## 2. Applied Research Methods

### 2.1. Condition monitoring system

In this research, the experimental protocol is based on the Condition Monitoring System (CMS). The data used is part of the online data protocol regarding the wind turbines' state of operation. The recorded data is analyzed using signal evaluation both in the time domain and in the frequency domain. The CMS provides all data sets as originally optimized for all turbines. The data is collected from a wind turbine gearbox. The repartition of the sensors in the monitoring process of the wind turbine from the actual stage of the research is shown in Figure 2.

The analysis is centered on the gearbox, examining the vibrations at three specific points of the gearbox: Low-speed Shaft (LSS), Intermediary Shaft (IS), and High-Speed Shaft (HSS). The data acquisition is conducted using vibration sensors fixed on the bearings of the kinematic chain, starting from the input, which is the rotor side, and extending to the output, which is the generator side.

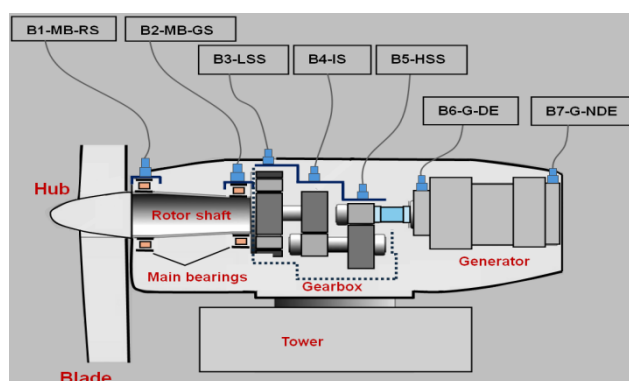
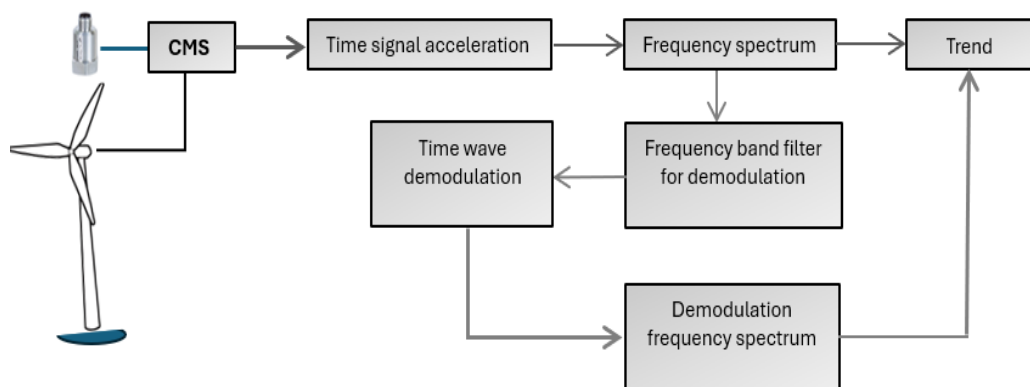


Figure 2. Schema of the experimental stand with the position of the used sensors.

**Table 1-** Sensors notation and position on the wind turbine

Sensor label	Description
B1-MB-RS	Main bearing accelerometer- rotor side
B2-MB-GS	Main bearing accelerometer- generator side
B3-LSS	Gearbox accelerometer- low-speed shaft
B4-IS	Gearbox accelerometer- intermediary shaft
B5-HSS	Gearbox accelerometer- high-speed shaft
B6-G-DE	Generator accelerometer drive end-side
B7-G-NDE	Generator accelerometer non-drive end-side

The data transmission and processing chain is described in Figure 3. The online acquisition system allows the data to be recorded according to the original settings thus capturing signals along with their speed and power readings. In this way, the evolution of vibrations can be determined specific to certain values of speed and power [20]. The system allowed the definition of parameters in the frequency domain both in the acquisition and analysis phases. The selected frequency range is according to ISO10816-21 standards, including the rotor, gearbox, generator, and tower/nacelle. Figure 3 shows the data sets according to CMS, for the gearbox in the 3 entry points, LSS, intermediate IS, and HSS.



**Figure 3.** Synopsis of data acquisition and signal processing.

In these experiments the data from the input of the gearbox, the acceleration in the frequency domain at LSS, and the data of the gearbox output, in the frequency domain at HSS is taken into account, figure 4.

		▲ Measuring time	Alarm	Reset	FFT	Alarm FF	Time sig	Characteristic	Attril	Conven	Speed/RPM	1. log Trigger/RPM	2. log Trigger/kW
LSS	Planetary stage (m/s <sup>2</sup> RMS)	12/20/2023 8:20:24 PM	Green				✓	✓			1208.984	1208.984	571.350
	Planetary stage (m/s <sup>2</sup> E RMS)	12/21/2023 4:27:18 PM	Green				✓	✓			1276.367	1276.367	666.809
IS	Planetary stage 3 (m/s <sup>2</sup> RMS)	12/22/2023 8:35:38 PM	Yellow				✓	✓			1659.180	1659.180	1861.450
	Planetary stage 3 (m/s <sup>2</sup> E RMS)	12/23/2023 8:40:40 PM	Green				✓	✓			1201.172	1201.172	578.369
HSS	Spur gear transmission stage (m/s <sup>2</sup> RMS)	12/24/2023 8:45:32 PM	Yellow				✓	✓			1270.508	1270.508	659.790
	Spur gear transmission stage (m/s <sup>2</sup> E RMS)	12/25/2023 8:49:24 PM	Green				✓	✓			1438.477	1438.477	1010.742
	Spur gear transmission stage (m/s <sup>2</sup> RMS)	12/26/2023 8:26:04 PM	Green				✓	✓			1258.789	1258.789	624.695
	Spur gear transmission stage (m/s <sup>2</sup> RMS)	12/27/2023 5:14:24 PM	Green				✓	✓			1202.149	1202.148	555.908
	Spur gear transmission stage (m/s <sup>2</sup> E RMS)	12/28/2023 8:26:49 PM	Green				✓	✓			1188.477	1188.477	546.082
		12/29/2023 6:18:14 PM	Green				✓	✓			1309.570	1309.570	699.097
		12/30/2023 5:57:03 PM	Green				✓	✓			1194.336	1194.336	557.312

**Figure 4.** Example of CMS data presentation.

### 2.2. Signal processing and defect detection

The experimental is based on real-time vibration monitoring, using National Instrument equipment cRIO-9076, with 12 input channels, 24 bits resolution and a 50kSamples/s/ch. max. speed, figure 5. The real time monitoring data is set on 25kSamples/s, a buffer size with 32768Samples and a block size with 10kSamples. The vibration monitoring provide the signal data from the 3 accelerometers fixed on the 3 gearbox points: the LSS with the

1-2 stages, the IS- the 3 stage and the HSS with the spur gear stage. The accelerometers used are with the 100mV/g sensitivity for the IS and HSS point and with 500mV/g sensitivivity for the LSS point. For a precise synchronization between vibration signals and speed signal, a laser speed sensor fixed at the generator side was used.

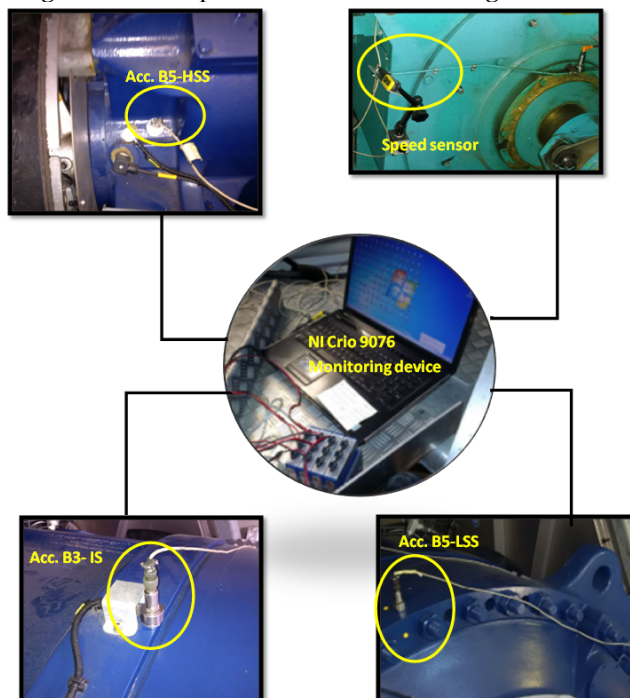


Figure 5. Vibration monitoring devices.

Signal analysis was done by numerical processing taking into account the parameters (frequency and amplitude) being monitored. Thus, Figure 6 shows the waveforms obtained with the help of the monitoring software both in the time domain and in the frequency domain and in figures 7 and 8 are shown acceleration signal in the case of the gearbox wear. The vibration parameters are set according to the ISO10816-21 standard, specifying acceleration in m/s<sup>2</sup> RMS, vibration velocity in mm/s RMS, and demodulated

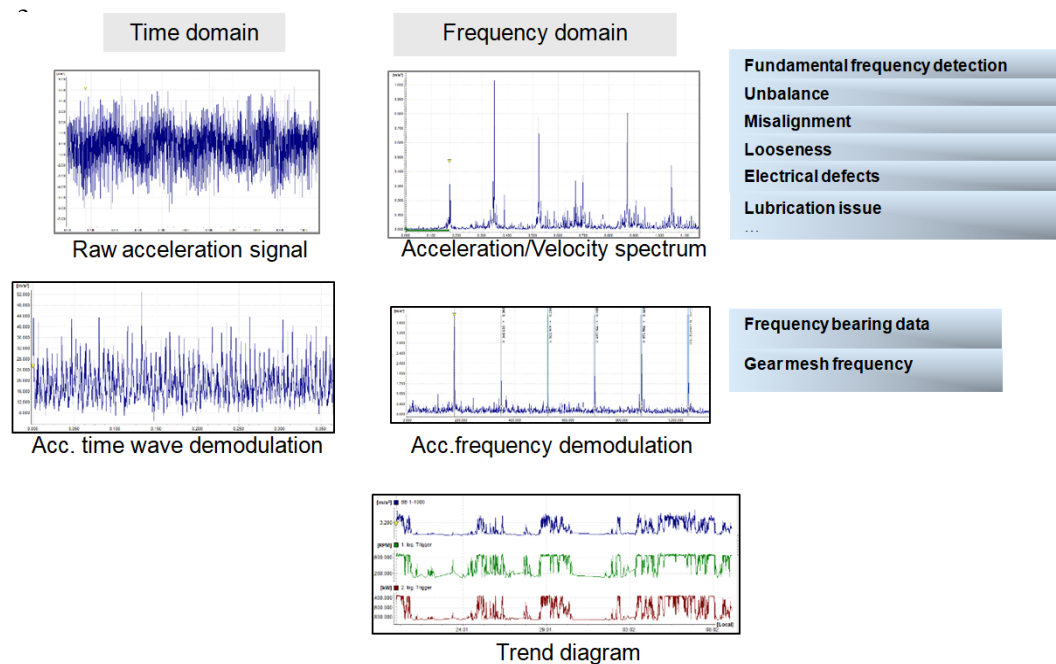
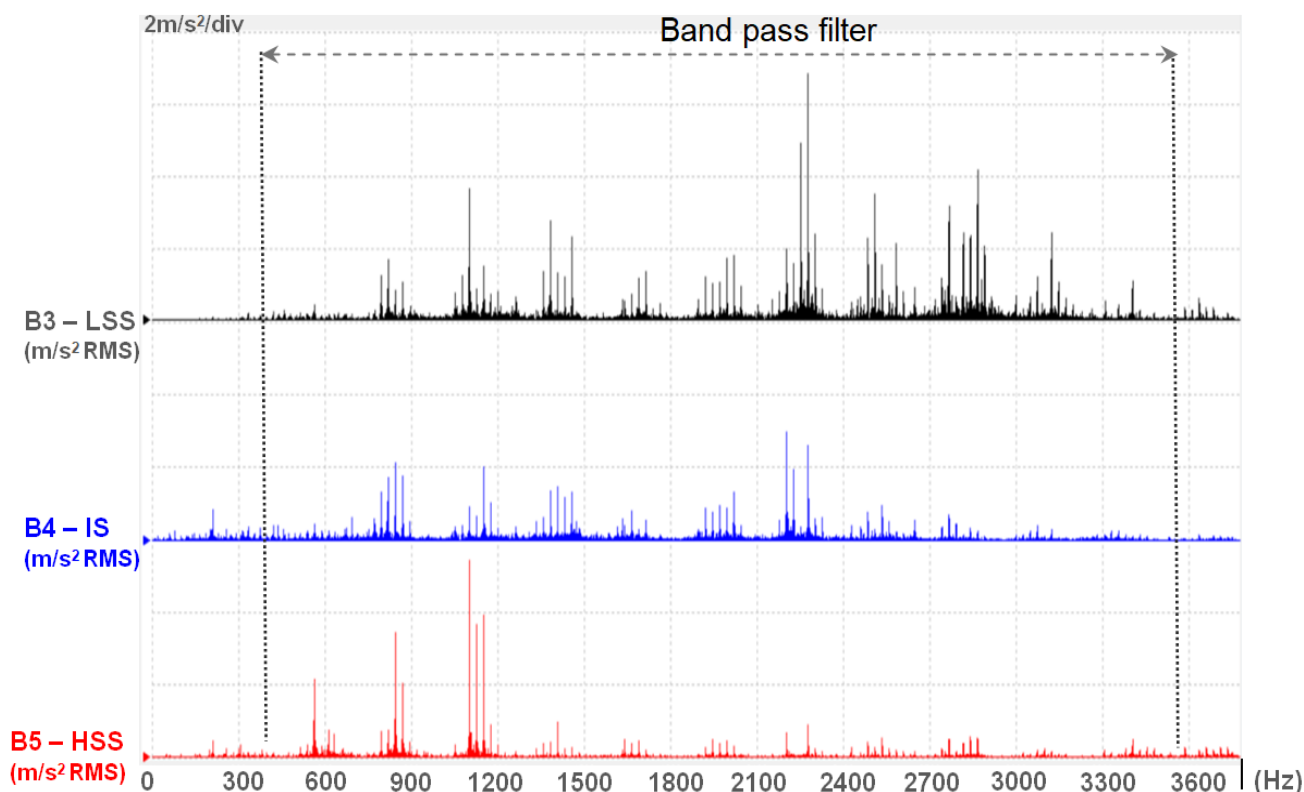


Figure 6. Signal processing and defect detection from CMS.

278 2E. With the bearing frequency data, the characteristic frequency of the bearing defect  
 279 can be identified. The structure of the vibration parameters is complex and based on the  
 280 vibration defect theory [21,22]. The vibration limits for wind turbines, provided by the  
 281 ISO standard 10816-21, present an integrated base defining the recommended state of  
 282 operation [23-25]. Even in this situation, many specific cases of vibration of the wind  
 283 turbine components are difficult to classify according to this standard [26]. For this  
 284 purpose, it is proposed to develop a model that can interpret the state of operation in  
 285 real operating conditions using data provided by CMS



286  
287 **Figure 7.** Acceleration signal in the case of the gearbox wear.

288 The processing data and analysis approach for bearing detection is applied also for gear  
 289 characterization by using the gear mesh frequency data according to the kinematic chain  
 290 of the gearbox [9-12]. The signal processing and analysis is performed with Fastview  
 291 software, which allows the use of both vibration monitoring and analysis in real time.  
 292 The software allows the identification of the specific failure frequencies of the gear and  
 293 bearings by the method of vibration demodulating using envelope function [27] with a  
 294 dynamic filtering of the specific domain frequencies (figure 7).

295 A novelty in the evaluation analysis of the gearboxes wear condition is the envelope  
 296 method using the Hilbert transform [27] with side bands energy coefficient integration,  
 297 called SER coefficient (Sideband Energy Ratio™, a patent pending algorithm utilized  
 298 in the General Electric) [28-30] so that the impact energy generated by the defect can be  
 299 quantified (figure 8).

300 Figure 8 shows the spectrum of the acceleration envelope in the case of the gearbox  
 301 defect. The quantification of the defective condition is evaluated by means of the gear  
 302 mesh frequency presence (GMF) in relation to the side bands, as well as its harmonics.  
 303 According to the quantification of the level of sidebands in relation to the amplitude of  
 304 the GMF frequency, it can be found that the ratio is less than one, which means that the  
 305 defect on the HSS stage is present, and is in an advanced state.



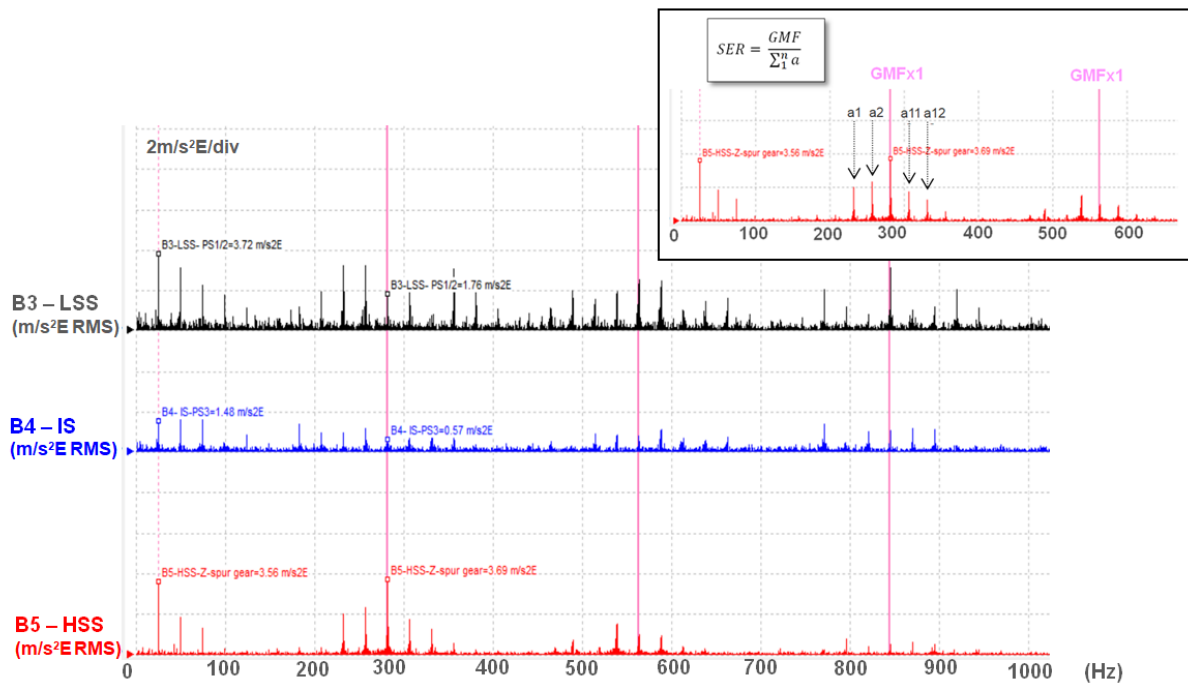


Figure 8. Envelope acceleration in the case of a gearbox wear.

### 2.3. Using BDSVM-Based Data Extraction Technique

The Base density of the Support Vector for Machine Learning (BDSVM) [30] has been beneficial in establishing the basic data for neural network learning. In any monitoring activity, it is more efficient to train the neural network using BDSVM as it reduces the learning input data (decreasing computational complexity) and determines the resulting weights matrices to identify a mechanical failure without being impacted by the outliers. This study exploits this method to find the most relevant data points and establish the objective function (FO).

This data extraction method is based on the filtering of data points based on their population density. Population density of data points refers to the correlation between the population size and the space they occupy. The rationale behind this data filtering is to deal with the data points that are influenced by random noises or gross errors. These data points do not accurately represent the general trend. These points are considered outliers and can affect the accuracy of the established objective functions and subsequently the analysis. The densely populated areas in the input space are determined by calculating the Mahalanobis distance (9). The points lying in this region are considered meaningful points while the points lying outside of this region are considered outliers.

The Mahalanobis distance is calculated from the quantity  $\mu$  which represents the average of the points' distances, to each point. The  $cov^{-1}$  represents the inverse covariance matrix. This distance is [33,34]. The Mahalanobis distance takes into account the correlation of the data set and does not depend on the measurement scale [34-36]. The population variance is calculated with a variance-covariance matrix [35]. The Mahalanobis distance from the point to the mean of the distribution  $\mu$  can be calculated by (9), and the Mahalanobis distance from one point to another can be calculated by (10):

$$d = \sqrt{(x - \mu)^T cov^{-1}(x - \mu)} \tag{9}$$

$$d = \sqrt{(x - y)^T cov^{-1}(x - y)} \tag{10}$$

Where the population variance is calculated with [12]:

$$\text{var}(x_n) = \frac{\sum_1^n (x-\mu)^2}{n} \quad (11)$$

and population covariance with:

$$\text{cov}(x_n, y_n) = \frac{\sum_1^n (x_i-\mu_x)(y_i-\mu_y)}{n} \quad (12)$$

If  $\text{cov}(x_i) \& \text{cov}(y_i) > 0$

both of them increase or decrease;

If  $\text{cov}(x_i) \& \text{cov}(y_i) < 0$

when  $x_i$  increases  $y_i$  decreases or vice-versa;

If  $\text{cov}(x_i) \& \text{cov}(y_i) = 0$

not exist any relation between  $x_i$  &  $y_i$ ;

If  $\text{var}(x_i) > \text{var}(y_i)$

$x_i$  increase or decrease faster than  $y_i$ ;

End.

The average of  $d$  is:

$$\text{average}_d = \frac{\sum_1^n \sqrt{(x_i-\mu)^T \text{cov}^{-1}(x_i-\mu)}}{n} \quad (13)$$

where  $d_i$  is the distance between the points and  $d$  is the average of these distances

If  $d_i > d$ ,

the point  $i$  is in the outlier group;

Else

the point  $i$  will be considered important (meaningful) points in BDSVM;

End.

#### 2.4. Objective functions

The optimization function (FO) was proposed as a polynomial function of the fifth order with real coefficients that will be constructed by using the data from the acquisition of Fourier spectrum of the vibrations:

$$FO = a_1 * x^5 + a_2 * x^4 + a_3 * x^3 + a_4 * x^2 + a_5 * x + a_6 \quad (14)$$

where  $a_i$  will be determined by using the matrix equation:

$$\begin{pmatrix} a_1 \\ a_2 \\ \dots \\ a_6 \end{pmatrix} = \left\{ \begin{bmatrix} x_1^5 & \dots & x_1 \mathbf{1} \\ \vdots & \ddots & \vdots \\ x_5^5 & \dots & x_5 \mathbf{1} \end{bmatrix} \begin{bmatrix} x_1^5 & \dots & x_1 \mathbf{1} \\ \vdots & \ddots & \vdots \\ x_5^5 & \dots & x_5 \mathbf{1} \end{bmatrix}^T \right\}^{-1} \begin{pmatrix} FO_1 \\ \dots \\ FO_5 \end{pmatrix} \quad (15)$$

with the following constraints:

-  $x_i > 0$ ;

-  $x_i$  must be meaningful points,  $x_i \in \text{group } 1$ ;

-  $x_i \in \text{BDSVM}$ ,

where  $FO_i$  is the amplitude of the vibration evolution in time where the defect will appear and  $x_i$  is the frequency in time. To define the FO, 5 boundary points  $(x_i, FO_i) \in \text{BDSVM}$  will be used for each moment of time vs. frequency points but under the same conditions of forced vibration and for the same wind turbine. The BDSVM points must strictly adhere to the condition of belonging to BDSVM which is that:

$$d_i < \text{average}_d. \quad (16)$$

The boundary of  $FO$  will be the limit of the optimal functioning of the wind turbine. In this way, the moment of time for intervention on the gearbox will be determined, to eliminate the danger of an imminent defect.

2.5. The used proper LabView virtual instrument for  $FO$

To solve the objective function  $FO$ , proper LabView virtual instrumentation was used and the block schemas are shown in Figures 9-11.

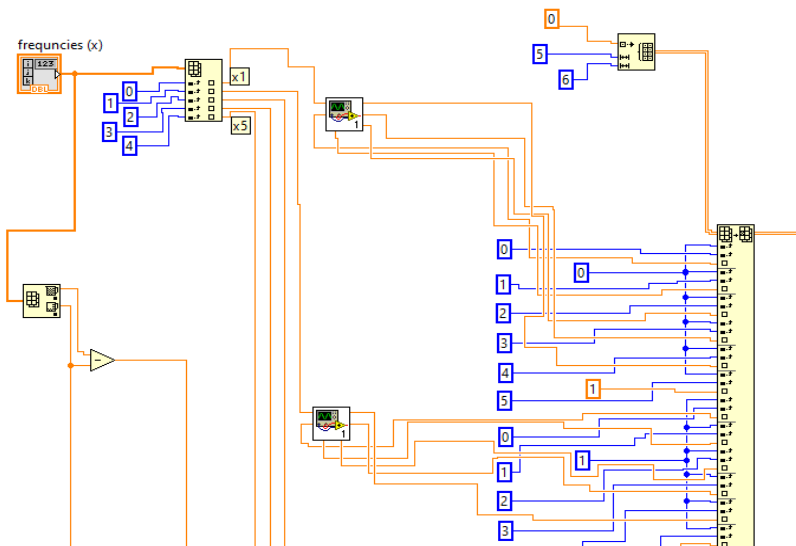


Figure 9. Part of the block schema of the LabView virtual instrument to determine the  $FO^5$  order.

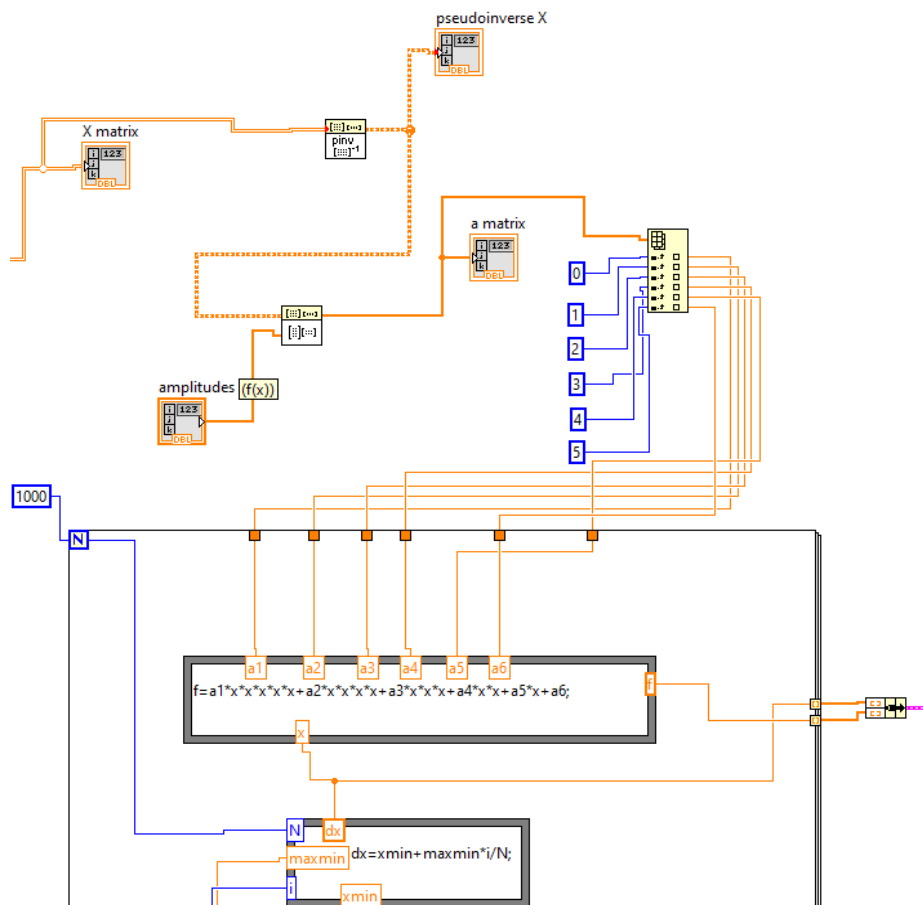
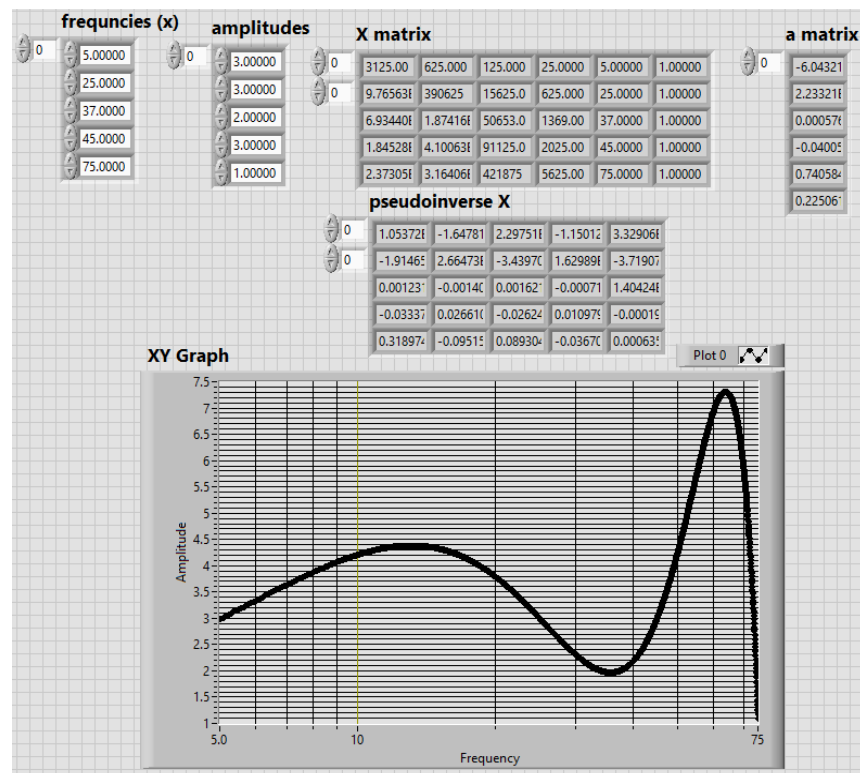


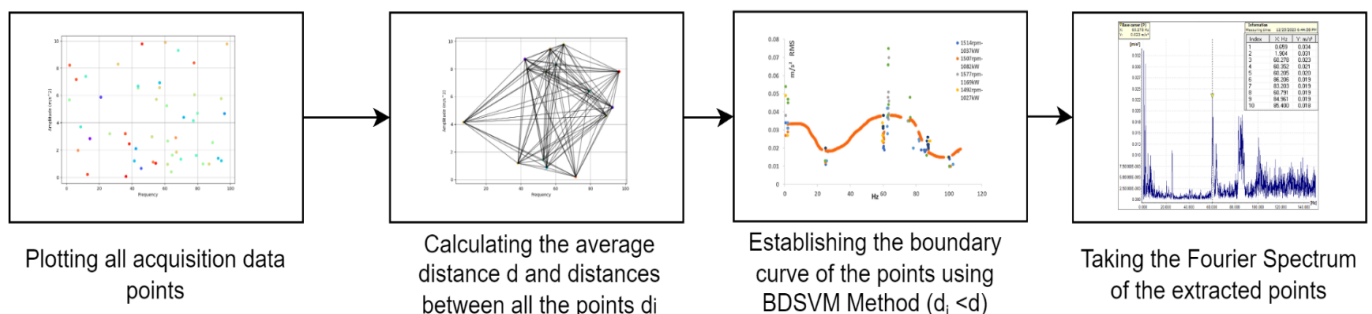
Figure 10. Part of the block diagram represents the  $FO$  (polynomial function of the 5-degree order) characteristic.



401 **Figure 11.** Front panel with the results of the optimization function  $FO$  for known points from the  $BDSVM$  (the  
 402 maximal values from the Fourier spectrum).  
 403

404 **2.6. Description of the used algorithm**

405 The used algorithm includes the following stages, as depicted in figures 12 and 13: (i)  
 406 acquisition of data at different moments of time, for the same parameters of wind,  
 407 power, speed; (ii) application of relation (12) for calculating the distances between points  
 408  $d_i$  (max. amplitude, frequency of the fourier spectra acquired); (iii) applying relation (13)  
 409 to determine the average distance,  $d$ ; (iv) defining group 1 of the  $BDSVM$  after checking  
 410 the condition  $d_i < d$ ; (v) establishing the boundary curve of  $BDSVM$ ; (vi) analysis of  
 411 Fourier spectra from group 1; (vii) defining the 5 maximum points from the Fourier  
 412 spectra both for the upwind position and for the downwind position of the sensors; (viii)  
 413 the use of LabView virtual instrumentation to determine the 5th order objective  
 414 functions; (ix) plotting multiple objective functions for Fourier spectra acquired during  
 415 three months of operation, under the same conditions of wind, power, speed; (x)  
 416 defining the maximum points of the objectively drawn functions, in order to determine  
 417 the trend; (xi) determining the coefficients of the 5th order objective functions of the  
 418 trend for both low and high frequencies, as well as for upwind and downwind of the  
 419 gear box sensors positions.



420 **Figure 12.** Block schema of the part of the used algorithm to establish the  $BDSVM$  of the collected data.  
 421

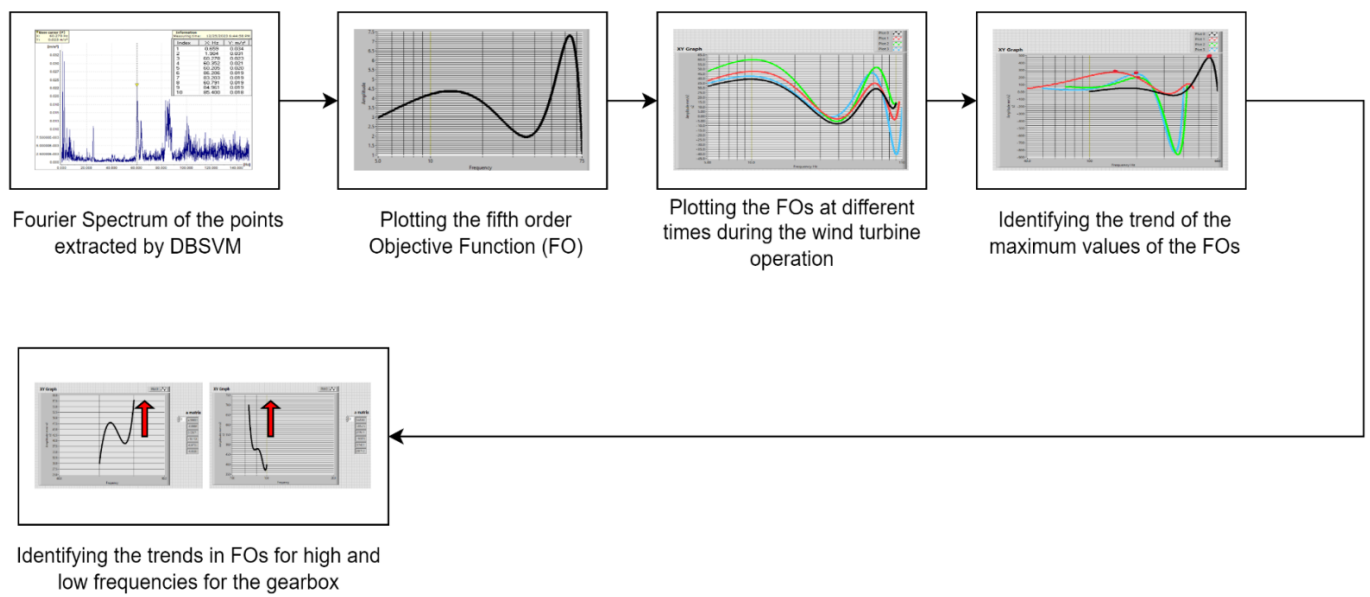


**Figure 13.** Block schema of the part of the used algorithm to establish the objective functions (FO) by using the Fourier spectrum collected from the boundary of the BDSVM.

### 3. Results and Analysis

#### 3.1. Establishing FO boundary of Fourier spectrum

If the operational limit of the turbine is set at a specific FO, a defect can be easily detected through control at each frequency. This can be done by checking if the operational point (frequency, magnitude) is in the normal functioning area or outside of this. In this way, it is possible to determine the maximum permissible magnitude of vibration.

In this case, the equation of the FO will be:

$$FO = -6.043x^5 + 2.233x^4 + 0.0005x^3 - 0.04x^2 + 0.74x + 0.225 \tag{17}$$

For predictive maintenance, the following relation would be applied:

$$FO_i(f_i) < FO_j(x_i) \tag{18}$$

where  $x_i$  is the frequency for the imposed five points  $\in$  BDSVM, the points from boundary limits, and  $f_i$  is the all current frequencies that must be checked. If this condition is false, the respective points could be the potential mechanical wear.

Using the Fourier spectra, the objective functions (FO<sub>i</sub>) were constructed the objective functions (FO<sub>i</sub>) for each of these data sets. All these FOs were shown in Figure 12-15, for upwind and downwind sensors from the wind turbine gearbox. All objective functions FO, were determined by using the maximal values of magnitude from each of the used Fourier spectra, see the table of each acquisition Fourier spectrum.

#### 3.2. Construct the objective functions FO for all selected Fourier spectra

To construct the FO for the data acquisition and establish the trend of the maximum values of the vibration magnitude vs. frequency were used four Fourier spectra for the upwind and downwind bearings, see Figure 15. The results of FO<sub>i</sub> are shown in Figures 16 and 18.

To validate the mathematical vibration model proposed (figure 13), the vibration data is obtained from the CMS of 2.0 MW industrial WT gearbox, based on the acceleration position and data acquisition shown in figure 2 and 5. The gearbox is planetary type with a transmissions ratio 116. This model was applied to synthesize the

data acquisition of the wind turbine in the period between December 2023 to February 2024. The conditions that were imposed are the following: (i) the data acquisition was for the same, or very similar wind turbines; (ii) the data acquisition was carried out from the sensors from the gearbox, B3-LSS, and B5-HSS, HSS upwind bearing radial and similarly HSS downwind bearing radial; (iii) the data acquisition was performed in the similar dynamic conditions of wind intensity, speed, and power; (iv) the acquisition data that was synthesized is the data that falls under the condition to be classified as a meaningful point,  $x_i \in \text{group } 1, x_i \in \text{BDSVM}$ , see figure 14.

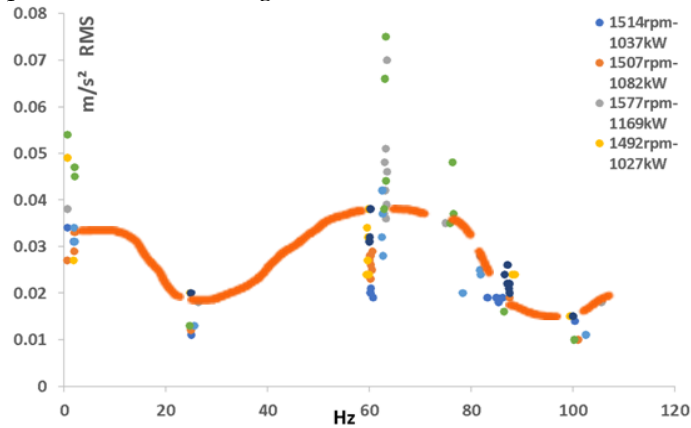
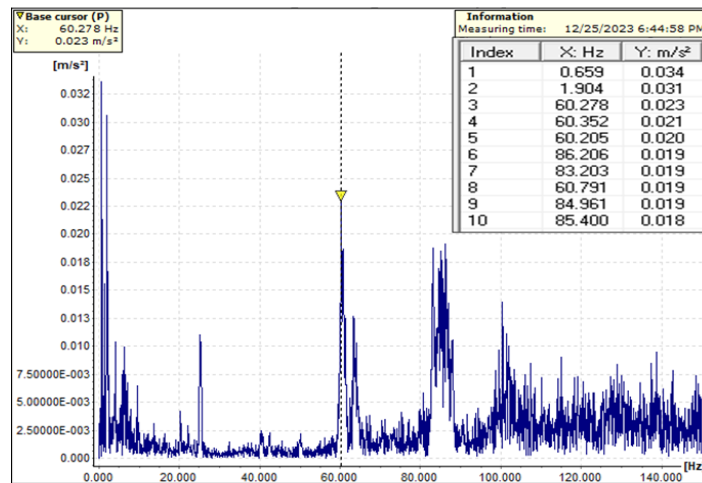
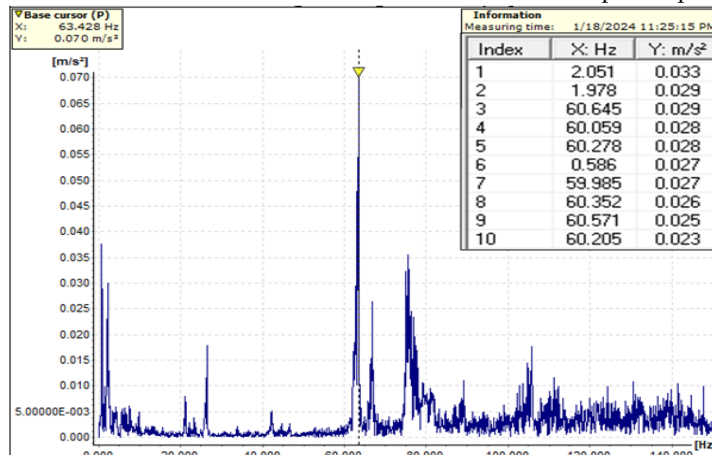


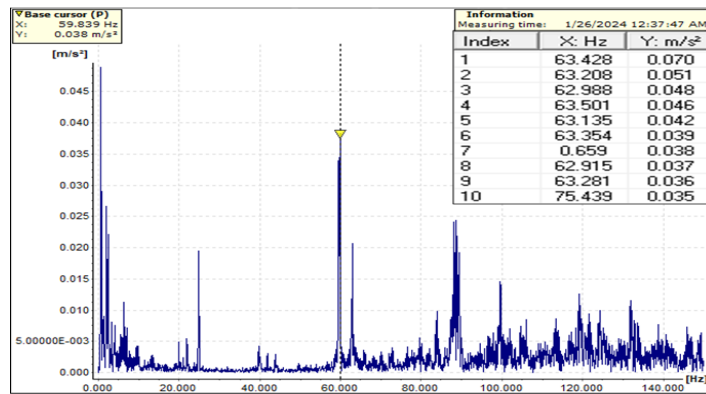
**Figure 14.** The acquisition data distribution and the establishment of boundary values for group 1, representing meaningful points of BDSVM, occur under similar dynamic conditions of speed and power. This characteristic is constructed by applying the BDSVM algorithm.



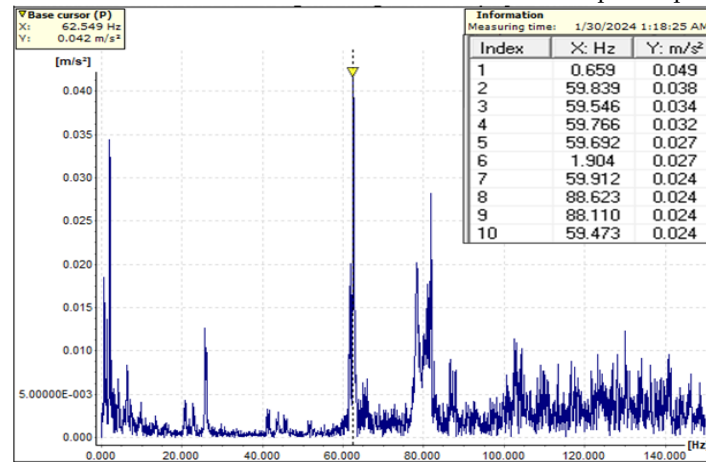
a- Fourier spectrum at 1514RPM and 1037.4kW on 25/12/2023, in an upwind position



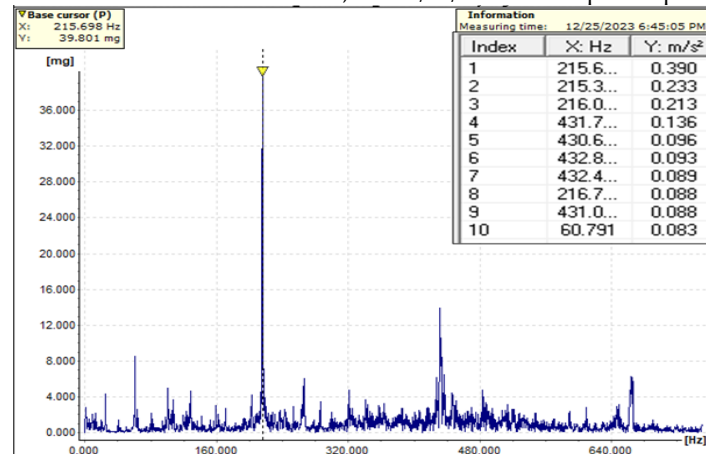
b- Fourier spectrum at 1577RPM and 1169.4kW on 18/01/2024, in an upwind position.



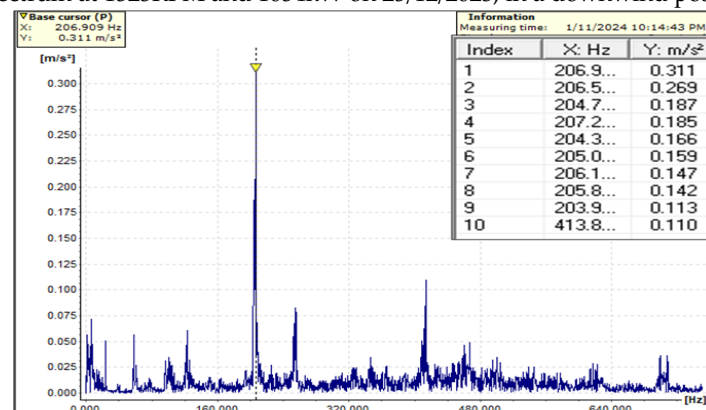
c- Fourier spectrum at 1492RPM and 1027.6kW on 26/01/2024, in an upwind position.



d- Fourier spectrum at 1552RPM and 1158kW, on 30/01/2024 in an upwind position.



e- Fourier spectrum at 1523RPM and 1054kW on 25/12/2023, in a downwind position.



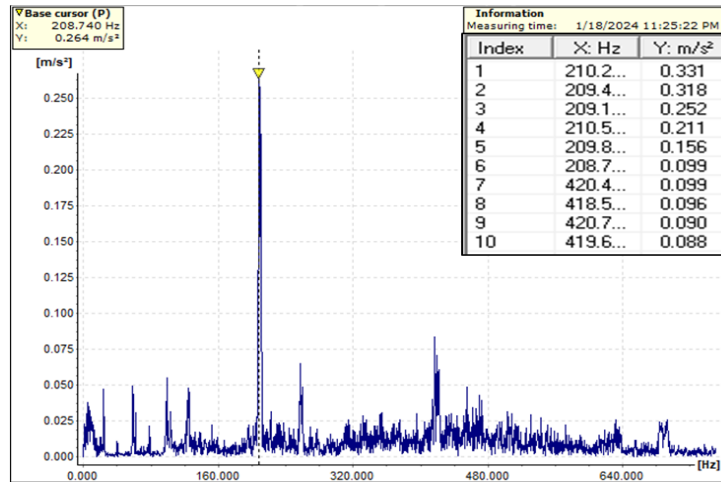
f- Fourier spectrum at 1455RPM and 971.4kW on 11/01/2024, in a downwind position.

474  
475

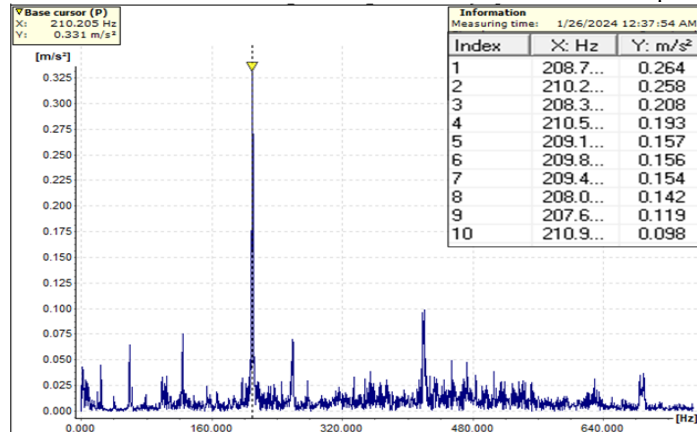
476  
477

478  
479

480  
481



g- Fourier spectrum at 1471RPM and 982kW on 18/01/2024, in a downwind position.



h- Fourier spectrum at 1481 RPM and 1006.5kW on 26/01/2024, in a downwind position.

Figure 15. Fourier spectrum from data acquisition between December 2023 to February 2024, in an upwind and downwind position of the sensors in the gearbox of WT.

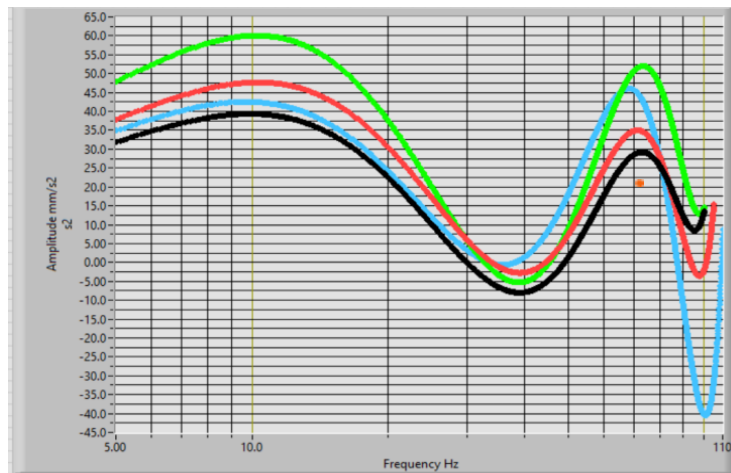


Figure 16. Objective functions ( $FO_i$ ) for all four selected acquisition data in the upwind sensor position. Using the data from the column matrices  $a_i$ , the fifth-order equation for  $FO_i$  will be determined. The  $FO_i$  for the upwind position of the sensor is shown in relation (19) and for the downwind position in relation (20).

$$FO = 6.64x^5 - 0.00017x^4 + 0.017x^3 - 0.0668x^2 + 8.84x + 2.473 \tag{19}$$

$$FO = 7.44x^5 - 0.0002x^4 + 0.019x^3 - 0.762x^2 + 10.368x + 2.921$$

$$FO = 9.291x^5 - 0.00025x^4 + 0.00246x^3 - 0.969x^2 + 13.1305x + 3.664$$

$$FO = 8.28x^5 - 0.00022x^4 + 0.02x^3 - 0.762x^2 + 9.781x + 2.735$$



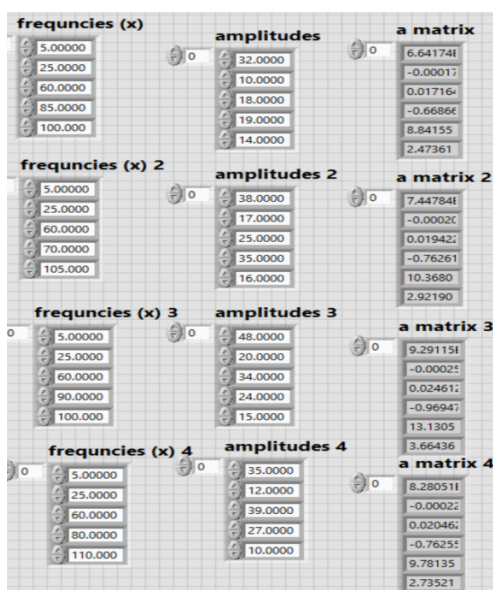


Figure 17. The front panel of the used LabView VI-s with input and output data for the upwind position sensor.

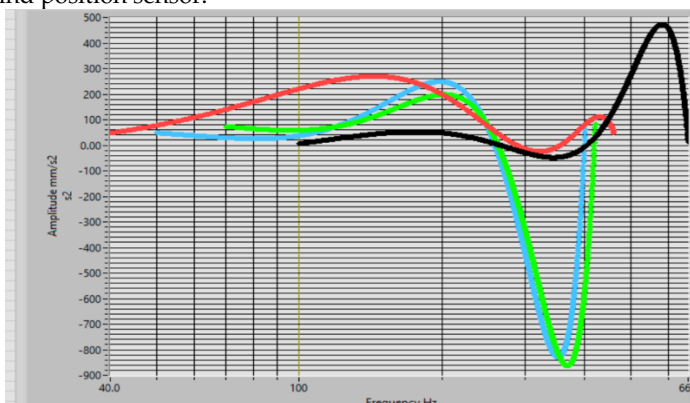


Figure 18. Objective functions (FO) for all four selected acquisition data in a downwind sensor position.

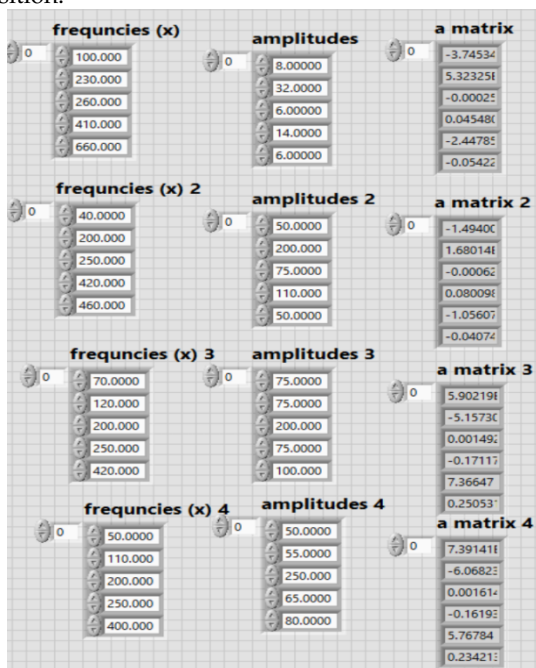


Figure 19. The front panel of the used LabView VI-s with input and output data for the downwind position sensor.

$$FO = -3.745x^5 + 5.323x^4 - 0.00025x^3 + 0.045x^2 - 2.447x - 0.054 \quad (20)$$

$$FO = -1.494x^5 + 1.68x^4 - 0.00062x^3 + 0.08x^2 - 1.056x - 0.04$$

$$FO = 5.902x^5 - 5.157x^4 + 0.00014x^3 - 0.171x^2 + 7.366x + 0.25$$

$$FO = 7.391x^5 - 6.068x^4 + 0.00161x^3 - 0.161x^2 + 5.767x + 0.234$$

All determined *FO*s represent different stages of the mechanical condition of the turbine gearbox assembly.

### 3.3. Determine the *FO* for the trend

With the help of these functions, the trend of potential defects in the turbine gearbox area can be assessed. The characteristic frequencies of the WT gearbox in the damage case are presented in the figure 20 and 21, corresponding to LSS-upwind and HSS-downwind. The frequency spectrum of acceleration for LSS – upwind position shows the fundamental frequency of planet pin (figure 20) and the frequency spectrum of HSS – downwind position, shows the existence gear mesh frequency (GMF) generated by the HSS pin gear and planet pin gear. In the case of a fault gear the amplitude is much higher, reaching up to 10 times higher than in the normal condition case.

At any given moment, it is possible to check if the function is approaching the period close to the appearance of a defect or not [37, 38]. Throughout this timeframe, it will be possible to examine whether the points (Frequency, Magnitude) fall within the first or last *FO* or between them, providing information on the proximity of a potential defect, as per relations (19) and (20). The trends of these functions are depicted in Figure 22, represented by the maximum of the *FO* for each of the cases.

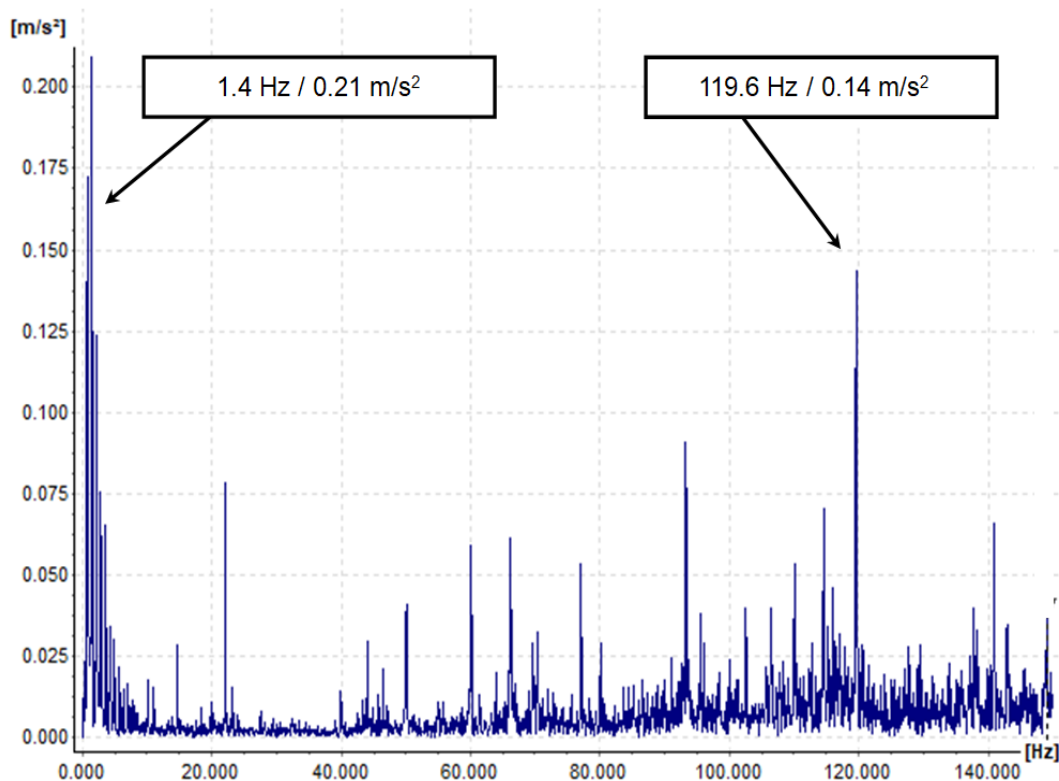


Figure 20. The frequency spectrum at LSS position in the case of gearbox defect.

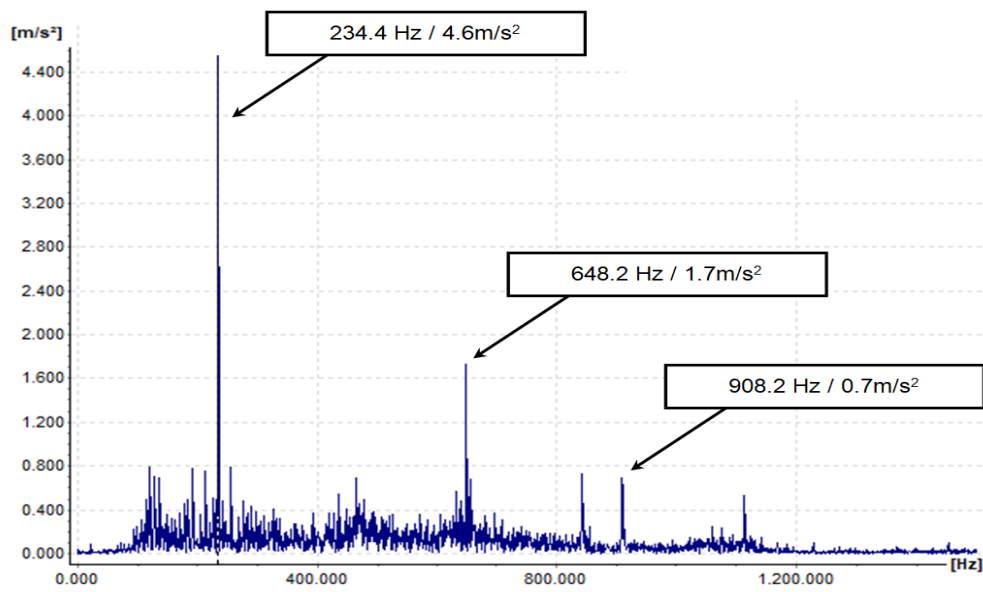


Figure 21. The frequency spectrum at HSS position in the case of gearbox defect.

The trend functions are the following:

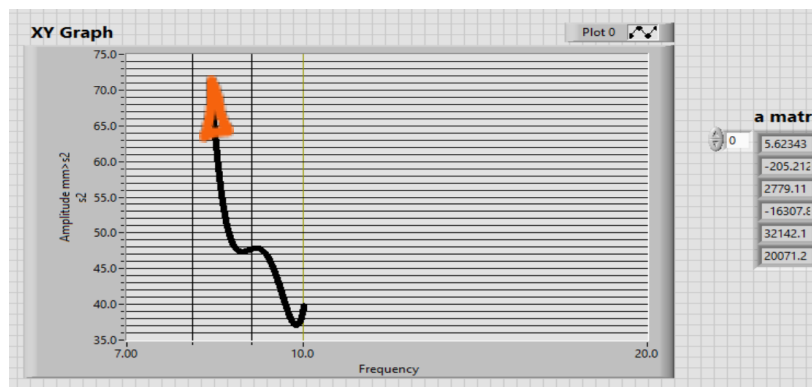
- for the low frequency in the upwind position  

$$FO = 5.6234x^5 - 205.21x^4 + 2779.11x^3 - 16307.64x^2 + 32142.12x + 20071.2$$
- for high frequency in the upwind position  

$$FO = 4.306x^5 - 0.0096x^4 + 0.7267x^3 - 18.112x^2 - 0.9755x - 0.0328$$
- for high frequency in the downwind position  

$$FO = -1.0703x^5 + 0.0086803x^4 - 2.6357x^3 + 355.109x^2 - 17907.9x - 451.047$$

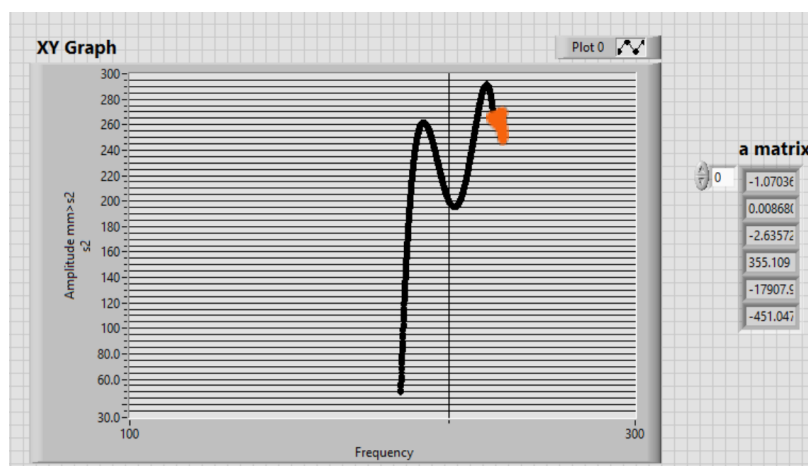
$$(Magnitude, frequency)_{i,catastrophic\ wear_{upwind\ or\ downwind}} \in FO_{trend_{upwind\ or\ downwind}} \tag{22}$$



a- Trend of the FO in the upwind position of the gearbox sensor in a low frequency.



b- Trend of the FO in the upwind position of the gearbox sensor in a high frequency.



c- trend of the *FO* in the downwind position of the gearbox sensor.

**Figure 22.** The trend of the magnitude- -frequency points from the *FO*.

If the first *FO* objective function is defined after an intervention when the gearbox is working correctly, and the last function is determined close to the appearance of a defect, the position of any point (frequency, amplitude) can be determined between these limits. Intermediate *FO*s define the intermediate limits. By using this method, it will be possible to implement preventive maintenance and also monitor the normal operation of the gearbox of the wind turbine. The validation of this developed method can be carried out by checking whether the maximum points (frequency, magnitude) from the Fourier spectrum belonging to a certain trend as identified by the objective functions, correspond to any known instances of gearbox malfunction or failure in wind turbines. This would be done through collaboration with a wind turbine expert.

#### 4. Conclusions and future work

This paper presents a novel approach to address the complexities of vibration monitoring and analysis in wind turbine gearboxes. By leveraging mathematical modeling and AI techniques, we have developed a method for evaluating gearbox conditions during operation that can help make meaningful interpretations from uncategorized vibration data from wind turbines. After analyzing the obtained results, the objective functions, and the trend of the monitoring results, we can make the following remarks: (i) The applied method is general and can be applied to many other dynamic monitoring processes; (ii) The designed LabView instrumentation for the synthetic analysis of the obtained acquisition data opens the way to applying more virtual instrumentation in monitoring the dynamic behavior across various mechanical fields; (iii) Using BDSVM to filter out the meaningful data adds a new front to applying machine learning in monitoring processes; (v) Establishing the trend of the *FO* for each position of the gearbox sensors ensures the design of an intelligent monitoring system for predictive maintenance; (vi) The trend for the low frequency in the upwind sensor position is a decrease in frequency and an increase in magnitude; (vii) conversely, the trend involves an increase in both frequency and magnitude for the high frequency; (viii) in the downwind sensor position, the trend is characterized by an increase in frequency and a decrease in magnitude.

In future work, we propose to generalize this method and leverage neural networks for the rapid establishment of weight matrices, objective functions, and wear trends in wind turbines across all sensors. This will be integrated into a comprehensive matrix comprising objective functions, alongside a monitoring and trend matrix.

In the next stage of this research SVM Regression analysis will be implemented to predict the magnitude of vibrations based on various input features (e.g., frequency,

time). This information will help obtain a quantitative measure of potential defects. Upon further assessment of the FFT spectrum of vibrations leading up to failures or defects, we also aim to study and explore other features (fluctuations in phase, etc.) that could indicate upcoming defects. This condition-based maintenance strategy can also be further enhanced by incorporating supervised classification. We plan to label the datasets indicating different points (labeled points) in time leading up to the developing fault. This would be done through collaboration with the industry specialists. The classification algorithm can be employed to identify the definite states of the system (normal operation, potential fault, critical fault). The combination of regression and classification would allow for a more comprehensive predictive maintenance approach. The proposed method is intended to be applied in other industrial applications in the case of condition monitoring of machine-tool spindles.

**Supplementary Materials:** Not applicable.

**Author Contributions:** Conceptualization, B.C. and O.A.; methodology, B.C. and O.A.; software, B.C. and O.A.; validation, B.C., O.A., O.S. and A.A.; formal analysis O.A., O.S., and A.A.; investigation, B.C., O.A., O.S., A.A., M.N. and U.H.; resources, B.C.; writing—original draft preparation, O.A. and B.C.; writing—review and editing, B.C. and O.A., O.S., A.A., M.N. and U.H.; supervision, O.A.; funding acquisition, B.C. and O.A. All authors have read and agreed to the published version of the manuscript.

**Funding:** This research received no external funding.

**Institutional Review Board Statement:** Not applicable.

**Informed Consent Statement:** Not applicable.

**Data Availability Statement:** The requested data is currently unavailable as the owner has deemed it confidential for economic reasons.

**Acknowledgments:** This work was supported by a grant from the National Program for Research of the National Association of Technical Universities - GNAC ARUT 2023.

**Conflicts of Interest:** The authors declare no conflict of interest.

## References

1. Yanyan Nie, Fangyi Li, Liming Wang a,b, Jianfeng Li, Mingshuai Sun, Mengyao Wang, Jianyong Li, A mathematical model of vibration signal for multistage wind turbine gearboxes with transmission path effect analysis, *Mechanism and Machine Theory* Volume 167, 2022.
2. F. Spinato, P.J. Tavner, G.J.W. Bussel, E. Koutoulakos, Reliability of wind turbine subassemblies, *IET Renew. Power Gener.* 3 (2009) 387–401.
3. C. Dao, B. Kazemtabrizi, C. Crabtree, Wind turbine reliability data review and impacts on levelised cost of energy, *Wind Energy* 22 (2019) 1848–1871.
4. Bo Ren, Yuan Chi, Niancheng Zhou, Qianggang Wang, Tong Wang, Yongjie Luo, Jia Ye, Xinchun Zhu, Machine learning applications in health monitoring of renewable energy systems, *Renewable and Sustainable Energy Reviews* 189, 2024.
5. S. Sheng and P. Veers, Wind Turbine Drivetrain Condition Monitoring – An Overview, *Mechanical Failures Prevention Group: Applied Systems Health Management Conference 2011 Virginia Beach, Virginia May 10 – 12, 2011.*
6. Yunyi Zhu, Bin Xie, Anqi Wang, Zheng Qian, Fault diagnosis of wind turbine gearbox under limited labeled data through temporal predictive and similarity contrast learning embedded with self-attention mechanism, *Expert Systems with Applications*, Volume 245, 1 July 2024.
7. W. Teng, X. Ding, X. Zhang, Y. Liu, Z. Ma, Multi-fault detection and failure analysis of wind turbine gearbox using complex wavelet transform, *Renew. Energy* 93 (2016) 591–598.
8. I. Vamsi, G.R. Sabareesh, P.K. Penumakala, Comparison of condition monitoring techniques in assessing fault severity for a wind turbine gearbox under nonstationary loading, *Mech. Syst. Signal Process.* 124 (2019) 1–20.
9. Teng, W.; Ding, X.; Tang, S.; Xu, J.; Shi, B.; Liu, Y. Vibration Analysis for Fault Detection of Wind Turbine Drivetrains—A Comprehensive Investigation. *Sensors* 2021, 21, 1686.

- 638 10. Libin Liu, Xihui Liang, Ming J. Zuo, Vibration signal modeling of a planetary gear set with transmission path effect analysis,  
639 Measurement, Issue 85, 2016, 20-31.
- 640 11. Xihui Liang, Ming J. Zuo , Libin Liu, A windowing and mapping strategy for gear tooth fault detection of a planetary  
641 gearbox, Mechanical Systems and Signal Processing, 80, 2016, 445–459.
- 642 12. Zhipeng Feng, Haoqun Ma, Ming J. Zuo, Vibration signal models for fault diagnosis of planet bearings, Journal of Sound and  
643 Vibration, 370, 2016, 372–393.
- 644 13. Tianyang Wang, Qinkai Han, Fulei Chu, Zhipeng Feng, Vibration based condition monitoring and fault diagnosis of wind  
645 turbine planetary gearbox: A review, Mechanical Systems and Signal Processing, 126, 2019, 662–685.
- 646 14. Jack P. Salameh, Sebastien Cauet, Erik Etien, Anas Sakout, Laurent Rambault, Gearbox condition monitoring in wind  
647 turbines: A review, Mechanical Systems and Signal Processing 111, 2018, 251–264.
- 648 15. Z. Hameeda , Y.S. Honga , Y.M. Choa , S.H. Ahnb, Condition monitoring and fault detection of wind turbines and related  
649 algorithms: A review, Renewable and Sustainable Energy Reviews 13 (2009) 1–39.
- 650 16. Mian Zhang, KeSheng Wang , Dongdong Wei, Ming J. Zuo, Amplitudes of characteristic frequencies for fault diagnosis of  
651 planetary gearbox, Journal of Sound and Vibration, 432, 2018, 119-132.
- 652 17. Brian McNiff, Jonathan Keller, Alfredo Fernandez-Sison, and Jens Demtröder A Revised International Standard for  
653 Gearboxes in Wind Turbine Systems. Presented at the Conference for Wind Power Drives Aachen, Germany March 21-22,  
654 2023.
- 655 18. Liang Cao and Shuangyin Liu, Vibration Suppression of an Input-Constrained Wind Turbine Blade System, Mathematics  
656 2023, 11, 3946. <https://doi.org/10.3390/math11183946>.
- 657 19. Jiale Peng, Yushu Bian, Dongbo Tian, Peng Liu, and Zhihui Gao, Vibration alleviation for wind turbine gearbox with flexible  
658 suspensions based on modal interaction, Journal of Low Frequency Noise, Vibration and Active  
659 Control Volume 42, Issue 3, September 2023, Pages 1390-1418.
- 660 20. Global Energy Research Council, Global Wind Report, 2009. [Online] [http://www.gwec.net/fileadmin/documents](http://www.gwec.net/fileadmin/documents/Publications/Global_Wind_2007_report/GWEC_Global_Wind_2009_Report_Lowres_15th.520Apr./pdf)  
661 [/Publications/Global\\_Wind\\_2007\\_report/GWEC\\_Global\\_Wind\\_2009\\_Report\\_Lowres\\_15th.520Apr./pdf](http://www.gwec.net/fileadmin/documents/Publications/Global_Wind_2007_report/GWEC_Global_Wind_2009_Report_Lowres_15th.520Apr./pdf).
- 662 21. T.W.Verbruggen, Condition Monitoring: Theory and Practice, 2009, *Wind Turbine Condition Monitoring Workshop*, October 8-9,  
663 2009, Broomfield, CO.
- 664 22. S. Sheng & P. Veers, Wind Turbine Drivetrain Condition Monitoring – An Overview, *Mechanical Failures Prevention Group:*  
665 *Applied Systems Health Management Conference*, 2011, Virginia Beach, Virginia, May 10 – 12, 2011.
- 666 23. Germanischer Lloyd, Guideline for the Certification of Condition Monitoring Systems for Wind Turbines, 2007, Hamburg,  
667 Germany.
- 668 24. T. Gellermann and G.Walter, Requirements for Condition Monitoring Systems for Wind Turbines, 2003, AZT Report  
669 no.03.01.068.
- 670 25. Wind Stats Newsletter, 2003-2009, vol.16, no.1 to vol.22, no.4, Haymarket Business, Media, London, UK.
- 671 26. P.Veers, Databases for Use in Wind Plant Reliability Improvement, 2009, *Wind Turbine Condition Monitoring Workshop*, October  
672 8-9, 2009, Broomfield, CO.
- 673 27. Claudiu Florinel Bisu, Miron Zapciu, Olivier Cahuc, Alain Gérard and Marin Anica, *Envelope Dynamic Analysis: A New*  
674 *Approach For Milling Process Monitoring*, The International Journal of Advanced Manufacturing Technology, Vol.62, Issue 5-8,  
675 pp 471-486, 2012.
- 676 28. Mian Zhang a b, Hao Cui c, Qing Li c, Jie Liu d, KeSheng Wang c, Yongshan Wang, An improved sideband energy ratio for  
677 fault diagnosis of planetary gearboxes, Journal of Sound and Vibration, Volume 491, 20 January 2021.
- 678 29. A Pattabiraman T.R.a, \*, Srinivasan K.b , Malarmohan K.b, Assessment of sideband energy ratio technique in detection of  
679 wind turbine gear defects, *Case Studies in Mechanical Systems and Signal Processing 2* (2015), 1–11.
- 680 30. J. Hanna, C. Hatch, M. Kalb, Detection of Wind Turbine Gear Tooth Defects Using Sideband Energy Ratio, GE Enregy,  
681 Nevada USA, 2012.
- 682 31. T. W. Verbruggen, Wind Turbine Operation and Maintenance Based on Condition Monitoring, 2003, Energy Research Center  
683 of the Netherlands, Petten, The Netherlands. [Online] [www.ecn.nl/publicaties/PdfFetch.aspx?nr=ECN-C--03-047](http://www.ecn.nl/publicaties/PdfFetch.aspx?nr=ECN-C--03-047).
- 684 32. Y.Dodge, *The Concise Encyclopedia of Statistics*, Springer 2008.
- 685 33. Z. Nazari, D. Kang, and H. Endo, Density Based Support Vector Machines, *The 29<sup>th</sup> International Technical Conference on*  
686 *Circuits/Systems, Computers and Communications (ITC-CSCC)*, pp.1-3, 2014.
- 687 34. El Moutaouakil K, El Ouissari A, Oлару A, Palade V, Ciorei M. OPT-RNN-DBSVM: OPTimal Recurrent Neural Network and  
688 Density-Based Support Vector Machine. *Mathematics*. 2023; 11(16):3555. <https://doi.org/10.3390/math11163555>.
- 689 35. Variance-covariance matrix- GeeksforGeeks.html.
- 690 36. Zahra Nazari and Dongshik Kang, “Density Based Support Vector Machines for Classification” *International Journal of*  
691 *Advanced Research in Artificial Intelligence (IJARAI)*, 4(4), 2015. <http://dx.doi.org/10.14569/IJARAI.2015.040411>.
- 692 37. Bo Ren, Yuan Chi, Niancheng Zhou, Qianggang Wang , Tong Wang, Yongjie Luo, Jia Ye , Xinchun Zhu, Machine learning  
693 applications in health monitoring of renewable energy systems, *Renewable and Sustainable Energy Reviews* 189, 2024.

- 694 38. Mohammad Valikhani, Vahid Jahangiri, Hamed Ebrahimian, Babak Moaveni, Sauro Liberatore, Eric Hines, Inverse modeling  
695 of wind turbine drivetrain from numerical data using Bayesian inference, Renewable and Sustainable Energy Reviews 171,  
696 2023.

697 **Disclaimer/Publisher's Note:** The statements, opinions and data contained in all publications are solely those of the individual  
698 author(s) and contributor(s) and not of MDPI and/or the editor(s). MDPI and/or the editor(s) disclaim responsibility for any injury  
699 to people or property resulting from any ideas, methods, instructions or products referred to in the content.